AFRL-OSR-VA-TR-2015-0229

DEVELOPMENT OF NEW GENERATION OF PERSPIREABLE SKIN

Patrick Kwon
MICHIGAN STATE UNIV EAST LANSING

02/20/2015
Final Report

Air Force Research Laboratory
AF Office Of Scientific Research (AFOSR)/ RTD
Arlington, Virginia 22203
Air Force Materiel Command

REPORT DOCUMENTATION PAGE

Form Approved
OMB No. 0704-0188

PLEASE DO NOT RETURN YOUR FORM TO THE ABOVE ORGANIZATION.

1. REPORT DATE *(DD-MM-YYYY)*	2. REPORT TYPE	3. DATES COVERED *(From - To)*
02-13-2015	Final Report	06/15/2010-11/14/2014

4. TITLE AND SUBTITLE

DEVELOPMENT OF NEW GENERATION OF PERSPIRABLE SKIN

5a. CONTRACT NUMBER

FA9550-10-1-0238

5b. GRANT NUMBER

5c. PROGRAM ELEMENT NUMBER

6. AUTHOR(S)

Patrick Kwon
Professor
Department of mechanical Engineering
Michigan State University
East Lansing, Michigan 48824

5d. PROJECT NUMBER

5e. TASK NUMBER

5f. WORK UNIT NUMBER

7. PERFORMING ORGANIZATION NAME(S) AND ADDRESS(ES)

Michigan State University

8. PERFORMING ORGANIZATION REPORT NUMBER

9. SPONSORING/MONITORING AGENCY NAME(S) AND ADDRESS(ES)

Air Force office of Scientific Research (AFOSR)

875 N. Randolph St.

10. SPONSOR/MONITOR'S ACRONYM(S)

11. SPONSOR/MONITOR'S REPORT NUMBER(S)

12. DISTRIBUTION/AVAILABILITY STATEMENT

DISTRIBUTION A: Distribution approved for public release.

13. SUPPLEMENTARY NOTES

14. ABSTRACT

This research work aims at the development of the autonomous, self-cooling multi-functional material systems. Similar to our skin that maintains our body temperature, the proposed material system will react to the external heat and open itself for the purpose of self-cooling. Thus, we have coined the term, 'Perspirable Skin.' The autonomous, self-regulating action of the skin comes from the inherent, unique capacity of each material in response to a temperature change. The wide spectrum of the changes in a variety of materials is harnessed to create the openings for self-cooling. This proposed work intends to explore the possibility of achieving the out-of the plane deformation that can expel a much larger volume of the compressed gas onboard, thus achieving the high capacity for self-cooling. When this happens, the compressed air blankets the surface to prevent frictional heating as a similar technology was found to be incredibly effective in permanent holes on turbine blade.

15. SUBJECT TERMS

16. SECURITY CLASSIFICATION OF:			17. LIMITATION OF ABSTRACT	18. NUMBER OF PAGES	19a. NAME OF RESPONSIBLE PERSON
a. REPORT	b. ABSTRACT	c. THIS PAGE			Patrick Kwon
X				17	19b. TELEPHONE NUMBER *(Include area code)* 517-355-0173

Reset

Standard Form 298 (Rev. 8/98)
Prescribed by ANSI Std. Z39.18
Adobe Professional 7.0

INSTRUCTIONS FOR COMPLETING SF 298

1. REPORT DATE. Full publication date, including day, month, if available. Must cite at least the year and be Year 2000 compliant, e.g. 30-06-1998; xx-06-1998; xx-xx-1998.

2. REPORT TYPE. State the type of report, such as final, technical, interim, memorandum, master's thesis, progress, quarterly, research, special, group study, etc.

3. DATES COVERED. Indicate the time during which the work was performed and the report was written, e.g., Jun 1997 - Jun 1998; 1-10 Jun 1996; May - Nov 1998; Nov 1998.

4. TITLE. Enter title and subtitle with volume number and part number, if applicable. On classified documents, enter the title classification in parentheses.

5a. CONTRACT NUMBER. Enter all contract numbers as they appear in the report, e.g. F33615-86-C-5169.

5b. GRANT NUMBER. Enter all grant numbers as they appear in the report, e.g. AFOSR-82-1234.

5c. PROGRAM ELEMENT NUMBER. Enter all program element numbers as they appear in the report, e.g. 61101A.

5d. PROJECT NUMBER. Enter all project numbers as they appear in the report, e.g. 1F665702D1257; ILIR.

5e. TASK NUMBER. Enter all task numbers as they appear in the report, e.g. 05; RF0330201; T4112.

5f. WORK UNIT NUMBER. Enter all work unit numbers as they appear in the report, e.g. 001; AFAPL30480105.

6. AUTHOR(S). Enter name(s) of person(s) responsible for writing the report, performing the research, or credited with the content of the report. The form of entry is the last name, first name, middle initial, and additional qualifiers separated by commas, e.g. Smith, Richard, J, Jr.

7. PERFORMING ORGANIZATION NAME(S) AND ADDRESS(ES). Self-explanatory.

8. PERFORMING ORGANIZATION REPORT NUMBER. Enter all unique alphanumeric report numbers assigned by the performing organization, e.g. BRL-1234; AFWL-TR-85-4017-Vol-21-PT-2.

9. SPONSORING/MONITORING AGENCY NAME(S) AND ADDRESS(ES). Enter the name and address of the organization(s) financially responsible for and monitoring the work.

10. SPONSOR/MONITOR'S ACRONYM(S). Enter, if available, e.g. BRL, ARDEC, NADC.

11. SPONSOR/MONITOR'S REPORT NUMBER(S). Enter report number as assigned by the sponsoring/ monitoring agency, if available, e.g. BRL-TR-829; -215.

12. DISTRIBUTION/AVAILABILITY STATEMENT. Use agency-mandated availability statements to indicate the public availability or distribution limitations of the report. If additional limitations/ restrictions or special markings are indicated, follow agency authorization procedures, e.g. RD/FRD, PROPIN, ITAR, etc. Include copyright information.

13. SUPPLEMENTARY NOTES. Enter information not included elsewhere such as: prepared in cooperation with; translation of; report supersedes; old edition number, etc.

14. ABSTRACT. A brief (approximately 200 words) factual summary of the most significant information.

15. SUBJECT TERMS. Key words or phrases identifying major concepts in the report.

16. SECURITY CLASSIFICATION. Enter security classification in accordance with security classification regulations, e.g. U, C, S, etc. If this form contains classified information, stamp classification level on the top and bottom of this page.

17. LIMITATION OF ABSTRACT. This block must be completed to assign a distribution limitation to the abstract. Enter UU (Unclassified Unlimited) or SAR (Same as Report). An entry in this block is necessary if the abstract is to be limited.

Final Report

DEVELOPMENT OF NEW GENERATION OF PERSPIRABLE SKIN

Contract Number AFOSR FA9550-10-1-0238

Patrick Kwon
Department of Mechanical Engineering
Michigan State University
East Lansing, Michigan 48824
pkwon@egr msu.edu
(517) 355-0173

EXTENTED ABSTRACT

This research work aims at the development of the autonomous, self-cooling multi-functional material systems. Similar to our skin that maintains our body temperature, the proposed material system will react to the external heat and open itself for the purpose of self-cooling. Thus, we have coined the term, 'Perspirable Skin.' The autonomous, self-regulating action of the skin comes from the inherent, unique capacity of each material in response to a temperature change. The wide spectrum of the changes in a variety of materials is harnessed to create the openings for self-cooling. In the previously funded program, this concept mainly has relied upon the in-plane deformations on the surface plane of the skin and has limited capacity for self-cooling. This proposed work intends to explore the possibility of achieving the out-of the plane deformation that can expel a much larger volume of the compressed gas onboard, thus achieving the high capacity for self-cooling. When this happens, the compressed air blankets the surface to prevent frictional heating as a similar technology was found to be incredibly effective in permanent holes on turbine blade. In particular, three approaches are being considered to create considerable out-of-plane deformations for high capacity of self-cooling; (1) Designed thermal deformation, (2) Buckling caused by thermal loading and (3) A hinged structure triggered by internal pressure. All of these approaches must work with the thermal gradient loading prevalent in such application. At the beginning of the project, the first approach has been undertaken with modest gain in the cooling capacity. Even though the second and third approaches required precision machining capacity - which the request for DURIP has been discouraged due to the budgetary constraint, we were able to work on the development of a material system for the second approach. In this approach, a set of ceramic titles were designed and fabricated, which were shrink-fitted within the opening of the near zero Coefficient of Thermal Expansion (CTE) material simulating Reinforced Carbon-Carbon Composites (RCC). These tiles made of different materials including highly complex gradient materials induce thermal-induced buckling loads among the tiles under a given thermal loading condition. These tiles were fitted together to make seamless connections among them just like the skin on re-entry vehicles. However, when heated, these tiles expand in certain directions and shrink in other directions, exerting forces on one to the others to cause buckling, which enable the perspirable skin to blow out the cooler air onto the surface for self-cooling. This report illustrates our effort to achieve the perspirable skin.

1. INTRODUCTION

The original 'Perspirable Skin' concept, which AFOSR has graciously funded through Grant No. FA9550-05-10202, mainly utilizes in-plane deformation, opens the interference between two distinct materials described as 'a peg in a hole.' Fig. 1 depicts the core shrink-fitted into the hole in the skin, where the interference is designed to open when heated externally. The external surface temperature is expected to be extremely high on a supersonic plane or a reentry vehicle such as Space Shuttle. The use of the materials with distinct Coefficients of Thermal Expansion (CTEs) enabled the designed skin to achieve the interference of about 0.1mm with the core radius of 1cm, which is then used to extract the compressed air onboard [1]. Thus, instead of the atmosphere air striking and heating the surface, it will be mixed with the onboard compress air as it is being extracted through the interference. This is the main mechanism behind the original perspirable skin concept.

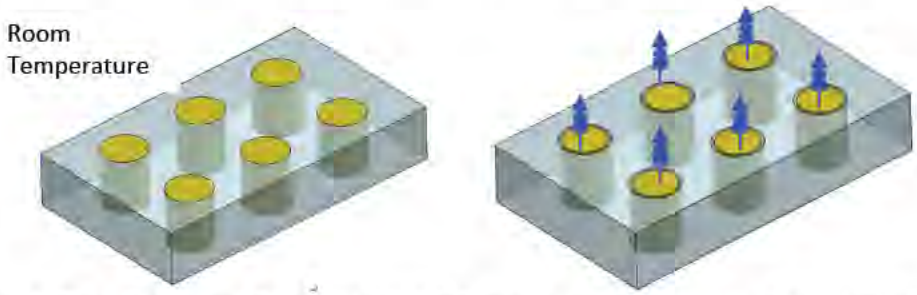

Figure 1: The 'Core and Skin with Hole' Concept of the Proposed Perspirable Skin

When the interference is closed, the aerodynamics of flying within the atmosphere will not be disrupted as the skin of the vehicle is the exactly same as the typical skin of such vehicle. However, during the reentry into atmosphere, it is know that certain locations of the skin are heated to extremely high surface temperature. The perspirable skin is placed in such locations where the interference between Core and Skin (as depicted in Fig. 1) is expected to open up at a designed temperature. The much simpler concept has been very successfully used in turbine blade. Small permanent holes on the surface of turbine blade are proven to be very effective to blanket the surface with cooler air as the hot combustible gas is introduced into the chamber. Here the stability of the turbine blade is not disrupted by the airflow from these holes. However, in the aerospace application, the vehicle stability may be seriously jeopardized if the aerodynamics changes due to these holes. The ideal solution is the 'skin' similar to our own. As our skin perspires to maintain our body temperature, the perspirable skin opens its 'pores' when the temperature reaches a critical temperature. Perspirable skin can be designed to have multiple interferences as shown in Fig. 1. The interference opens between the skin and cores when the surface reaches a designed temperature. Due to the limitation of small dimensions imposed on this design, however, the gap between the core and RCC was not big enough to achieve a high rate of cooling.

To achieve a higher capacity for self-cooling, three new design approaches have been considered; 1) Designed thermal deformation, (2) Buckling caused by thermal loading and (3) A hinged structure triggered by internal pressure. As stated, the second approach was the most viable solution based on the given experimental capability. To induce buckling action, an assembly of design shapes (called 'tiles') is designed and fabricated, which buckle under an expected thermal loading. These tiles had uniquely

designed CTE variations, where each tile pushes other tiles in certain directions while shrinking in other directions to enable buckling to occur under a given thermal loading. Finite Element Analysis (FEA) was performed with a set of possible material properties for a feasibility study. A major effort has been made to fabricate the designed tiles, some with anisotropic and/or gradient material properties. This document also reports on the development of processing techniques. Several samples were made successfully by compacting, pre-sintering, machining and fully sintering ceramic powders and powder mixtures.

2. BACKGROUND

Because of the high temperature applications, we are considering preferably many oxide ceramics and, to conform to the current technology with Space Shuttle, RCC composites with silica coatings. However, the same technology is applicable in any temperature range as long as the temperature change is large enough to allow the adequate in-plane or out-of-plane deformation. Oxide ceramics such as mullite, alumina and zirconia are considered because of oxidation resistance and the higher tensile strength. In this project, the CTEs of these materials are mostly critical. The application such as the skin for re-entry vehicle calls for a different kind of design as the heating of the skin occurs only on limited area of the skin. For such case, the core materials with negative CTEs such as zirconia tungstate (ZrW_2O_8 or ZT) [2-5] and the skin material with near zero CTE such as RCC [6] are being considered. Figure 2 also contains the CTE as a function of temperature of few materials that are distinct for their negative CTEs [2-5].

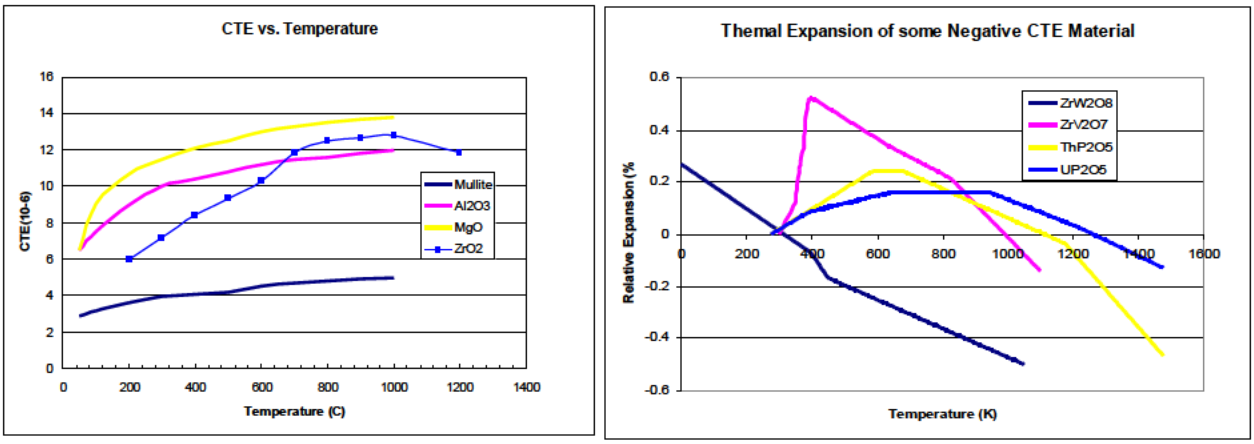

Figure 2: Temperature Dependency in CTE

The CTE of ZT is reported to be as low as -13.5×10^{-6}/°C between 298 and 428K and at -4.9×10^{-6}/°C [5] between 430K and 950K [7]. When the negative CTE materials is used in conjunction with RCC composites which have near zero CTE, the interference between NCTE material and RCC composite can be formed. With the RCC with near zero CTE, the core shrinks to open the interference. However, because ZT completely dissociates at 1230°C, the overheating of the ZT core must be avoided. The CTE of the ZT measured using the TMA in our lab is similar to the reported value. Despite of the low level of decomposition of ZT at 780°C, the use of ZT is feasible because the quenching delays the decomposition. The level of decomposition abruptly accelerates beyond 1000°C. The XRD testing of ZT after quenching shows that no microstructural changes have occurred.

These ceramics are the essential ingredients in the making of the proposed perspirable skin. In the previous project, the ceramics with negative CTE is essential in opening the interference when heated as most materials expand and push surrounding materials. As demonstrated in the next section, these materials – both positive and negative CTE materials – must be arranged to deliver the out-of-plane motion.

3. DESIGN APPROACHES

This proposed work (AFOSR Grant No. FA9550-10-1-0238) will explore a new out-of-plane deformation concept for 'Perspirable Skin' in order to achieve a much higher capacity for self-cooling. High capacity for self-cooling comes from the design of a medium to generate large but controllable out-of-plane deformations, enabling much larger air passage. Three new design approaches have been considered; 1) Designed thermal deformation, (2) Buckling caused by thermal loading and (3) A hinged structure triggered by internal pressure. Three approaches must work under thermal gradient loading expected in the application and are presented in the subsequent sections.

3.1 Designed Thermal deformation

Figure 3 represents the first approach where thermal deformation achievable by designing the deformable material surrounding the core as shown in Fig. 3(a). Because of the typical thermal gradient loading, the deformable material is expected to be the Functionally Gradient Material (FGM). The core made of FGM must be designed to bulge up as shown in Fig. 3(b) or bulge down under a typical thermal gradient loading. The top surface is expected to be in a high temperature while the bottom surface is expected to be at a lower temperature. Using this intense thermal gradiency, the gradiency in the core must be designed for the core to deform so that the cooling air can come out for self-cooling. It is expected to be very complex to design as well as to fabricate the core with the required gradiency. Based on the design iterations undertaken based on the FGM concept, the improvements (mainly the size of opening) we were able to attain were slightly higher than the original in-plane design.

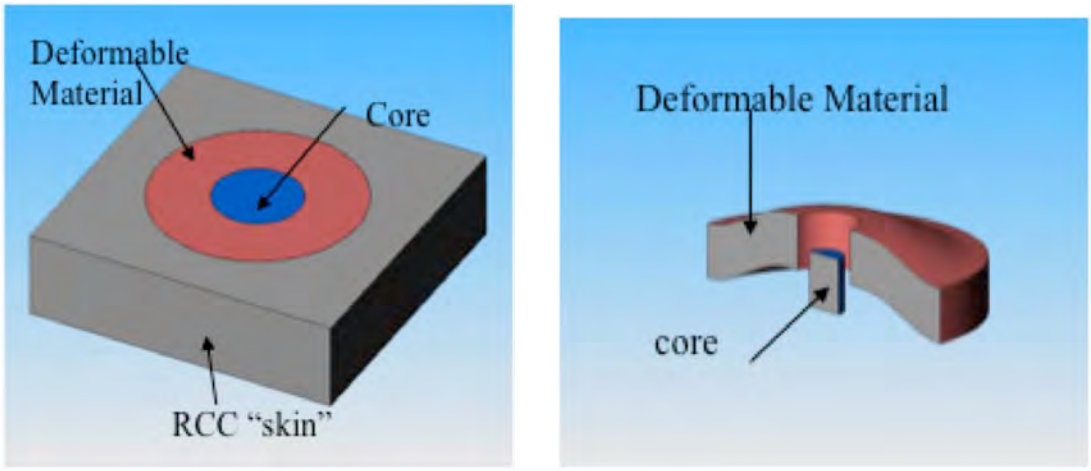

(a) Before loading (b) After loading

Figure 3: Deformable Materials under a given thermal gradient loading

3.2 Buckling caused by thermal loading

Figure 4 represents the second approach where the thermal buckling is achievable with a set of tiles. These tiles, shown in blue in Fig. 4(a), had uniquely designed CTE gradients, where each title pushes other tiles in the radial while shrinking in the circumferential direction to enable buckling to occur under a given thermal loading. The designed tiles are made of various materials with positive (e.g.: ZrO_2 or ceramic fibers) and negative (e.g.: ZrW_2O_8) CTEs. To confirm the viability of the buckling action, a series of FEM simulations was performed using ABAQUS. For our preliminary design analysis, the material properties were calculated using either the rules of mixture or the inverse rule of mixture along with the volume weighted average of the phases' (matrix and dispersed phase) properties [8]. With a volume ratio between ZrW_2O_8 and ZrO_2 of 7:3, the material properties used in our simulation were calculated using rule of mixture (longitudinal direction) or Inverse rule of mixture (transverse direction) and presented in Table 1.

Table.1. Material properties for the simulation

Using Simple ROM/IROM	Radial	Circumferential
CTE (/°C)	5.4e-6	-6e-6
Thermal conductivity (W/m/K)	5.6	2.7
E (MPa)	15.92	5.63
Poisson's ratio	0.3	

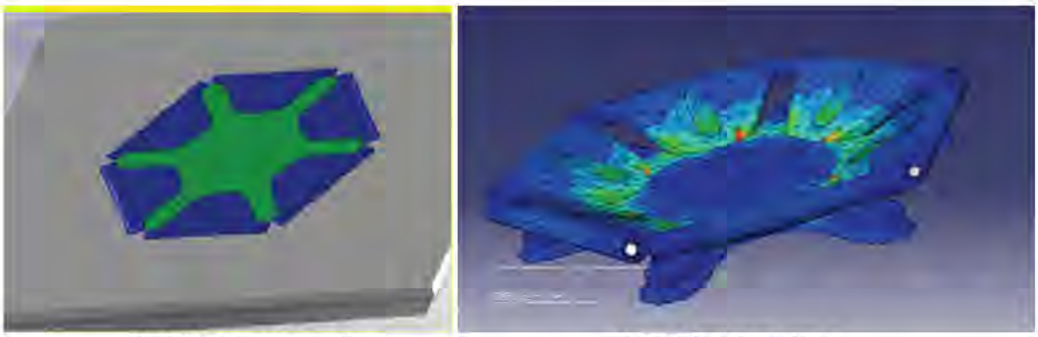

(a) Before loading (b) After loading

Figure 4: A set of tiles to **buckle** under thermal loading

The material for the core tile (shown in green on Fig. 3(a)) was imposed with a positive CTE of 3e-6. In the FEM simulation, the loading condition imposed was 800°C at the top surface and 50°C at the bottom surface. Concerning the boundary conditions, each tile had its own axis of rotation, which was fixed to the surrounding RCC. As the temperature of the perspirable skin increases due to the external heat, the tiles and the core will try to expand causing radial forces. With typical materials, the tiles will be constrained by the expansion in the circumferential direction. However, the tiles have the negative CTE in the circumferential direction, allowing the tiles to move against the core. It is not necessary for the CTE of the core to less than the CTE of the tiles as the size of the tiles is larger than the size of the 'finger' of the core. Thus, if the temperature continues to increases, the radial forces will reach high enough to buckle. These radial forces will put

the assembly in equilibrium due the hexagonal shape of the perspirable skin. With such loading and boundary conditions, the simulation has been carried out and confirmed that the designed assembly of tiles buckle as shown in Fig. 4(b). The buckling action is shown in Fig. 4(b) without the RCC skin.

New design with more simplified geometries is obtained due to the processing issue as shown in Fig. 5. The green parts are made of ZT which has negative CTE while the gray parts are made of ZrO2 which has positive CTE. Fig. 5(a) shows the top surface of the core while Fig. 5(b) shows the bottom surface of the core. Fig. 5(c & d) shows the core before and after ZrO_2 has been shrink-fitted. The tiles are shown in Fig. 5(e, f & g) (e without ZrO_2 and f & g in two views after ZrO_2 has been shrink-fitted.

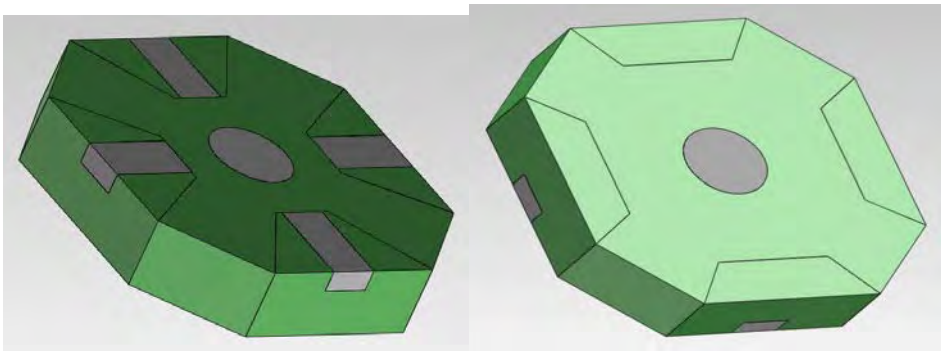

(a) Top Surface (b) Bottom Surface

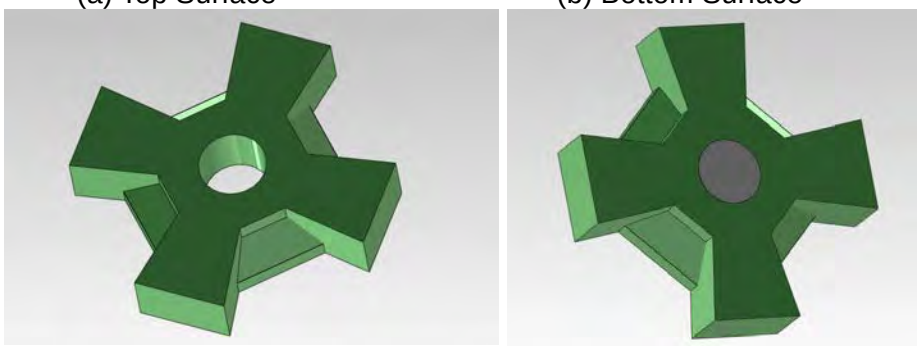

(c) Core (d) Assembled Core via Shrink-fit

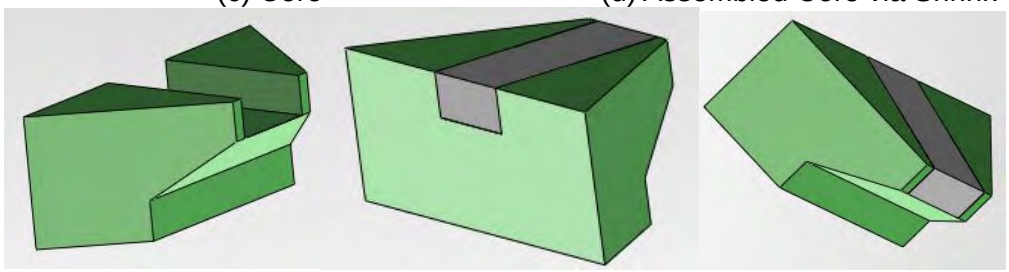

(e) A Tile made of ZT (f) Tile after fitting ZrO2 (g) Another view of (f)

Figure 5: New Design of Core and Tiles.

The stresses on ZT parts at the buckling temperature were simulated; the maximum principal stress was about 600MPa and the minimum principal stress was less than 100MPa depending on exact geometry. One instance of the principal stresses is presented in Figure 6. Because the failure stress is not known at high temperature for ZT, it will be hard to conclude the integrity and more work on ZT is required.

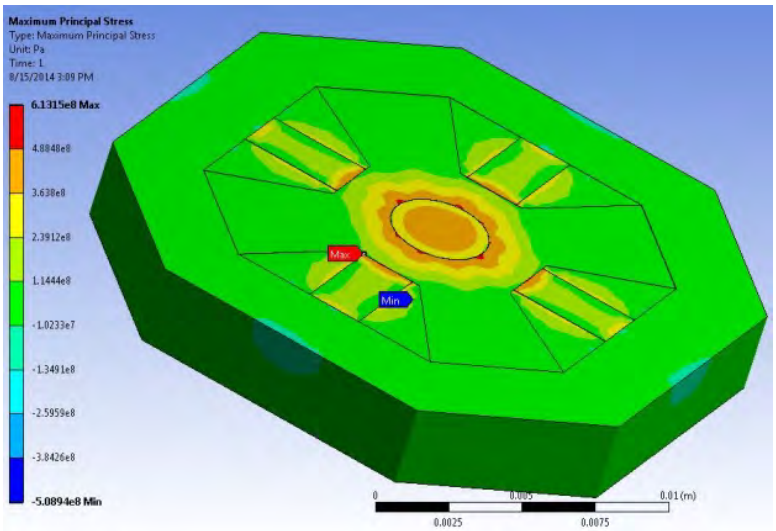

Figure 6: Principal Stresses at the Buckling Temperature

3.3 A hinged structure triggered by internal pressure

Finally the last approach requires the hinged structure where a set of tiles rotating around the hinges on the core shown in green in Fig. 7(a and b). The special material with near zero and negative CTEs [2-5] has a unique opportunity to serve on such design. As the hinged tiles shown in yellow in Figure 6 are made of slightly negative CTE and isotropic materials. The hinges between the core shown in green and the surrounding skin can be designed to rotate with the internal pressure of the air inside. The core may have to be connected to the skin to prevent the collapsing of the structure. As the hinged tiles shrinks due the temperature rise and the internal pressure will press the bottom surface of the hinged tile, the bottom surface can be modulated to rotate the tiles. When that happens, the perspirable skin will be reconfigured to the picture shown in Figure 7(b).

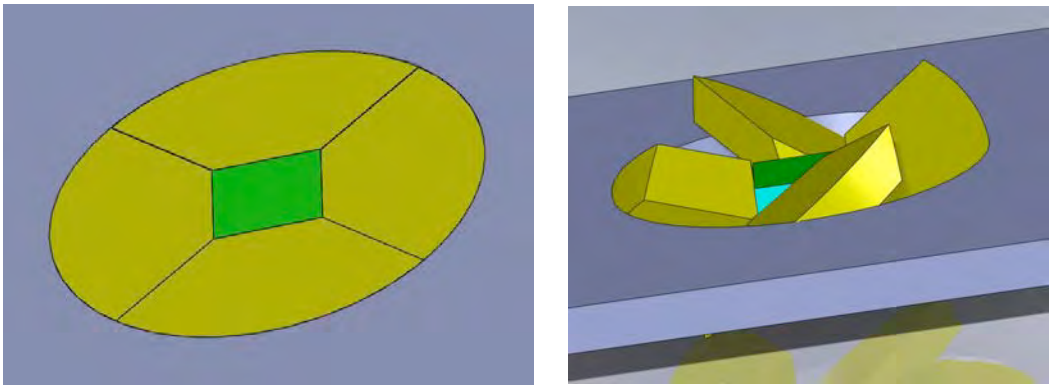

(a) Before loading (b) After loading

Figure 7. A hinged structure triggered by internal pressure

This design approach is possible as the CTE of a material can be tailored by mixing a

right volume ratio of ZrO2 and ZrW_2O_8 including a material with zero CTE [9]. Various mixtures of these compounds can be fabricated to control the shrinkage to make the perspirable skin of this type. FEM-based design processes were performed confirming the possibility. However, the machining facility required for the machining precisely design titles is unique as the partially sintered ceramics break into the powders instead of chips. These hard ceramics powder can be detrimental to the CNC machines as similarly happening in fabrication of the second approach as well. However, the precision required for this approach is incredibly high which our CNC machine could not provide. Thus, we gave up on pursuing this approach.

4. Development of Processing Techniques

4.1 Materials

According to the simulation results, the tiles with CTEs varying in at least two directions are needed to produce the buckling. While the CTE in one direction should be positive, the CTE in another direction needs to be negative. This negative CTE allows each tile to be free to move against others. Two methods of producing anisotropic/gradient materials are presented in Fig. 8. The first method combines ceramic powders with ceramic fibers. With the fibers arranged radially, a positive CTE can be obtained along the fiber direction. However, this approach was not successful due to the reaction and residual stresses created during sintering. Alternatively, arranging ZrO_2 and ZrW_2O_8 into certain shapes and sintering them together, creating a solid tile, can lead to different CTEs along different directions throughout the tile. Several ceramic powders and fibers that were used are shown in Table 2. As presented in Fig. 8(b), the CTE values are expected to change radially (e.g.: CTE=CTE(θ)). For example, when θ=0° as the elliptical shape becomes thinner, the CTE will be highly negative. On the other hand, when θ=90°, the CTE will attain the most positive CTE value. This meets the design requirement for the tiles presented in Figure 4.

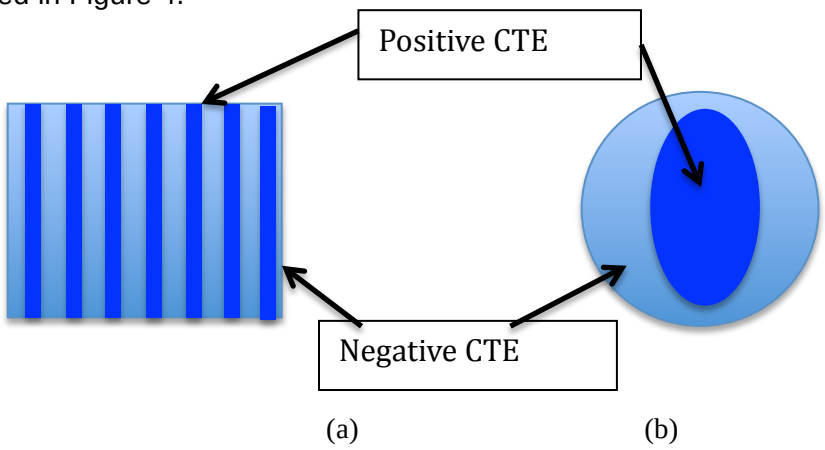

Figure 8. Processing (a) ceramic powders with fibers; (b) FGM in radial direction.

4.2 Procedure

4.2.1 Combination of ceramics and fibers

The WO_3+ZrO_2 powder mixture was mixed in a jar mill for 48 hours. The powder mixture with the stoichiometric ratio of WO_3 and ZrO_2 of 2:1 was prepared to attain pure ZrW_2O_8 [10]. With a small trace of Al_2O_3 powder, the final density of ZrW_2O_8 was improved [11]. Before mixing the powder with fibers, the fibers were heated to 600°C for two hours to

remove the organic sizing [12]. The mixture was then stacked in a single-action die and chopped fibers were placed along one direction. The mixture was then compacted under 70MPa of pressure.

Green compacts were then sintered at 1150°C for 6 hours in a covered platinum crucible under the atmospheric pressure in a furnace (Carbolite-HTF1700, UK). The crucible provides a nearly sealed environment, which is essential to reduce the sublimation of WO_3 at temperatures higher than 800°C [14]. Since decomposition of ZrW_2O_8 occurs when the temperature drops below 1100°C, a quenching process, performed by removing the crucible from the furnace at the end of the soaking stage, provides rapid cooling and prevents the decomposition from occurring at a lower temperature.

Table.2. Characteristics of Raw Powders and Fibers used

Name	Material	Mean particle size (μm)	Manufacturer
W-Fluka	WO_3	8.22	Sigma-Aldrich, U.S.A.
CERAC-2003*	ZrO_2	1.23	CERAC Inc., U.S.A.
Nextel 610	Al_2O_3	½" chopped fiber	3M company
SCS-6	SiC	142	Specialty Materials, INC.

4.2.2 Shrink-fitting Process to fabricate the assembly of ZrO_2 and ZrW_2O_8

Apart from the fabrication of the fiber-reinforced ZrW_2O_8, a shrink-fitting technique was used to fabricate the designed perspirable skin shown in Fig. 1. From our previous work [13], we were able to make continuous FGMs made of ZrO_2 and ZrW_2O_8. However, the processing technique was limited to produce the gradiency in one direction (through-the-thickness) only. The arrangement shown in Fig. 4(b) provides anisotropy in a composite-like manner. With short chopped fibers arranged various ways within a matrix, a complex gradiency can be achieved. However, as will be shown in Sec. 4, the processing of these materials presented many problems.

Alternatively, the arrangement shown in Fig. 5(a, b) can be the tile used for the simulation in Fig. 4(b). However, for simplification purposes, a simple circle has been used instead of the tile shape shown in Fig. 1. The tiles denoted positive CTE and negative CTE can be the FGMs produced in our previous work [9]. The denoted positive and negative CTEs mean the macroscopic CTE of each FGM tile. Fig. 2(b) is capable of achieving a wide variety of CTEs radially depending on the shape of the tile denoted positive CTE. We have not optimized the shape at the point. However, the designed shape behaves similarly as the tile used in our simulation shown in Fig. 1. To make the tile into the shape shown in Fig. 1, two methods were considered. One method was to make the sample using certain dies with the specific dimensions of the design's shape, and the other method was to machine the sample after partially sintering, and then fully sinter it to obtain the final product. The latter method was utilized to make the multidimensional material, since it was very inconvenient to design specific dies for each sample.

The overall processing technique is presented in Figure 9. The WO_3+ZrO_2 powder mixture was first partially sintered at 950°C for four hours, and subsequently CNC-milled, in order to obtain a certain shaped cavity in which a ZrO_2 tile was shrink-fitted. The ZrO_2 tile was partially sintered at 900°C for three hours, and then was machined into a

designed shape. After machining, the sample was fully sintered under 1350°C for four hours and then inserted into the ZrW_2O_8 tiles. These two tiles were co-sintered at 1150°C for 3 hours. By controlling the dimension of each part during partial-sintering and subsequent full sintering, the shrink-fit process has produced a successful assembly when considering the combination of ZrW_2O_8 shrinkage and ZrO_2 expansion during the sintering process. A reaction layer was formed at the boundary between the ZrW_2O_8 and ZrO_2, which is helpful in bonding these two materials together. Despite of the reaction, TMA measurements indicate that the macroscopic CTEs are maintained. The processed tile will function properly.

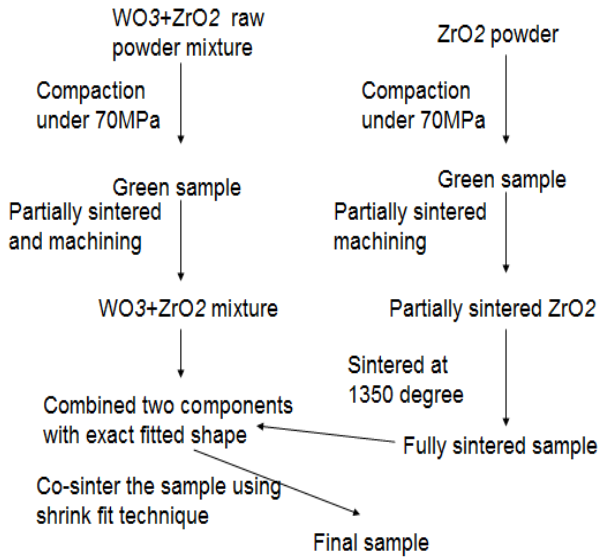

Figure 9. The Overall Processing Technique for shrink-fitting samples

The samples produced based on the procedure outlined in Figure 8 are presented in Figure 9. Figure 9(a) is a simple version of our sample that did not require the machining of the ZrO_2 tile. ZrW_2O_8 was partially sintered, on which a hole was drilled. After 3 hours of co-sintering, the sample was shrink-fitted together by placing the fully sintered ZrO_2 into the hole drilled into the partially sintered ZrW_2O_8 disk.

Two obvious phenomena should be reported. From our previous paper [13], the ZrO_2 powder will undergo a reaction with WO_3+ZrO_2 mixture during the sintering process. As shown in Figure 10(a), instead of the pure white color for the ZrO_2 powder, the core part has a yellow ring surrounding it, which is a mixture of ZrO_2 and ZrW_2O_8. Therefore, a functionally graded material was generated from the surrounding pure ZrW_2O_8 and the mixture of ZrO_2 and ZrW_2O_8 surrounding the pure ZrO_2. This FGM (the core part shown in Figure 10(a)) helps to join the two parts together. Adjusting the sintering temperature and soaking time can control the thickness of the reaction layer. The reaction layer is acceptable as long as the macroscopic CTEs are maintained.

Another important observation is the white spots on the ZrW_2O_8 tile. This is mostly due to the sublimation of WO_3 during the partial sintering and full sintering process, since it is known that the WO_3 powder will diffuse above 800°C. Therefore, the remaining ZrO_2 powders are the white spots shown on the surface. The sample shown in Figure 10(b) is the right tile shape used in our simulation shown in Figure 3. Both ZrO_2 and ZrW_2O_8 were partially sintered and machined. The key part of this process is that we need to compensate the size change during the partial and full sintering processes.

Then, the ZrO_2 sample will just fit into the shape after being fully sintered. The reaction layer cannot be observed on Figure 8(b) as the shrink-fit process has not taken place.

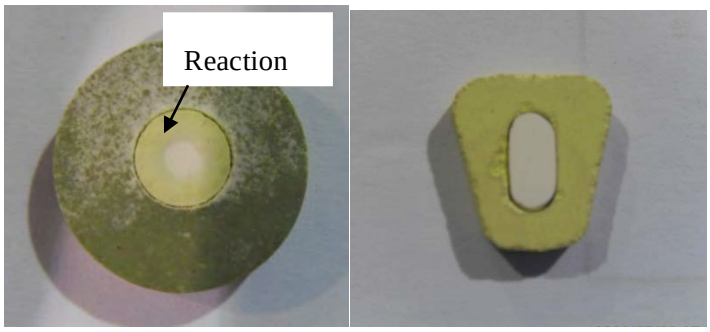

(a) (b)

Figure 10. Shrink-fitting samples: (a) simple one with a ring shape; (b) a designed shape model to simulate the tile part in the simulation

As presented with Figure 4(a), the CTE along the major axis of the elliptical shape is positive while the CTE along the minor axis is negative. Given the material properties, the extent of the radial CTE variation is strictly a function of the exact shape of the ellipse. The elliptical shape was determined to match the CTE values presented in Table 1. Using the processing techniques described above, we have made the perspirable skin as shown in Figure 11.

Figure 11: Fabricated Core and Tile and assembled Perspirable Skin on RCC (obtained from ADD, South Korea)

5. Results and discussion

Concerning the combination of ZrW_2O_8 with fibers, it was found that Al_2O_3 fibers undergo a chemical reaction with WO_3 when the temperature is higher than 720°C [15]. This compound exists in a liquid phase above 1135°C, which destroys the shape of the sample. Therefore, because Nextel 610 was mostly composed by Al_2O_3, it was found to be unfit for our purposes.

SiC fibers are very stiff and stable. During the sintering process, SiC fibers also react with the WO_3+ZrO_2 mixture, and become a liquid mixture at temperatures over 1200°C. However, at a temperature of 1150°C, the sample maintains its shape, as

shown in Figure 12. The CTE value measured from the sample was found to be -5.5X10^{-6}, which is a slight increase of 1.5 X10^{-6} compared with pure ZrW_2O_8. However, if we add more fibers to the mixture, the compaction of the green sample becomes a problem due to the stiffness of the SiC fibers, and the residual thermal stress due to the different CTE values will destroy the sample during the sintering process. Although there is no evidence of a chemical reaction between these two materials in our sample, the SiC fibers were not considered further.

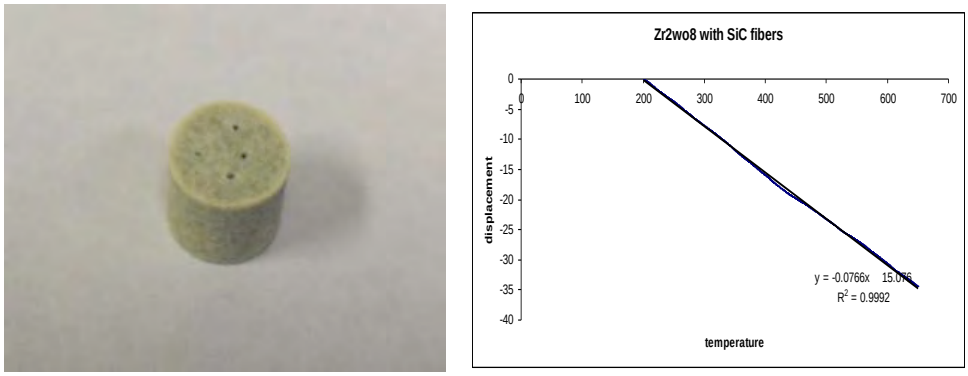

(a) (b)

Figure 12. Results for ZrW_2O_8 with SiC fibers: (a) sample; (b) CTE measurement data

Each of tiles is a homogeneous material but collectively they will behave like inhomogeneous materials. However, we are planning on making each tile in continuous FGMs as we have successfully made individually [14]. The FGMs made in [14] are extremely difficult to make as those have one material on one side and the other material on the other side, causing residual stress high enough to damage the sample.

Processing of ZT has been difficult to achieve near full density. Initially the main effort has been made to acquire higher density ZT by mixing additional smaller powders which can intestinally located themselves among larger powders. In addition to W-Fluka and CERAC-2003, Table 3 shows the powders used for this experiment. Mainly additional nano-powder for WO_3 were added to achieved denser ZT. As shown Figure 13, as the content of nanopowder increases, the final density increases until reaches the optimum point. However, after that, the final density did not improve. The trace of the other two TMDAR and MAGCHEM 10-325 were added as sintering aids to improve the final density. By adding only 0.4w% of sintering aids (Al_2O_3 and MgO), 96% of theoretical density was achieved.

Powder Name	Material	Mean Particle size (μm)	Manufacturer
W-Fluka	WO_3	8.22	Sigma-Aldrich, USA
Nano-Powder	WO_3	~0.66	Inframat Advanced, USA
CERAC-2003	ZrO_2	1.23	CERAC Inc., USA
TMDAR	Al_2O_3	0.17	Taimei Chem. Co., Japan
MAGCHEM 10 -325	MgO	0.25	MARTIN MARIETTA, USA

Table 3: Raw Powders Used In the Processing of ZT

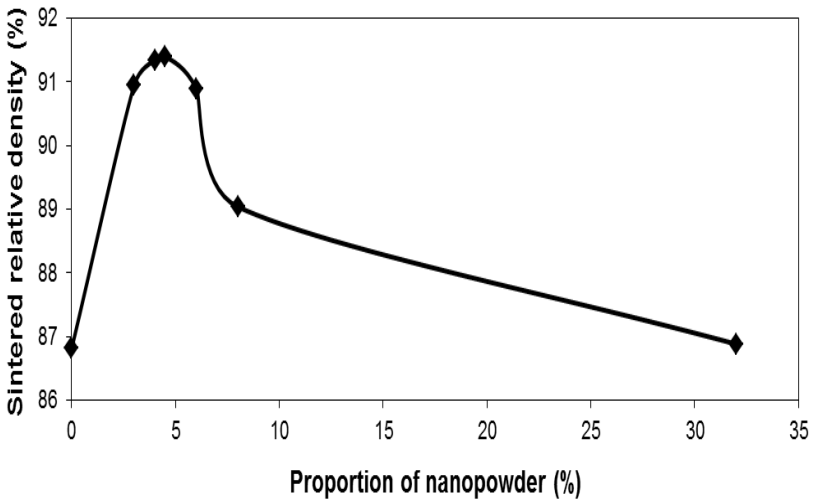

Figure 13: The Proportion of nanopowder in the ZT mixture and the final densities

The composite of void and ZT were also studied. We have also studies the micromechanics models using Mori-Tanaka (MT) Scheme using the following equation

$$\mathbf{C_{ef}} = \mathbf{C_m} + v(\mathbf{C_i} - \mathbf{C_m})\mathbf{A_i}$$

where $\mathbf{C_m}$ and $\mathbf{C_i}$ are the stiffness tensors of the matrix and inclusion materials as pores, respectively, v is the volume fraction of the inclusion phase. $\mathbf{A_i}$ is the inclusion strain concentrator tensor. Because ZT has inherent porosity, two MT schemes were predicted based on the pore as a second phase as well as the pore as matric materials. The elastic modulus was measured experimentally using 3-point bending test in order to make the comparison. Figure 14(a) shows the complete results of Elastic modulus. Figure 14(b) presents the CTE results, both experimental data and MT-scheme prediction. The experimental data of CTE were obtained using TMA procured through DURIP support in 2005.

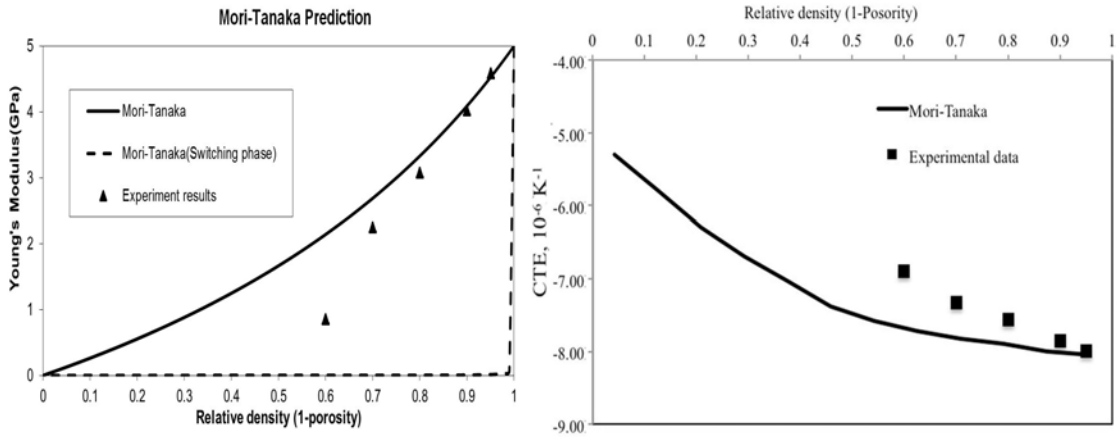

(a) Elastic Modulus (b) Coefficient of Thermal Expansion

Figure 14: M-T schemes with experimental data

PI has been also studied the 3DP in order to achieve the structural integrity of 3DP parts based on PI's previous work [16]. Additional work was conducted in 2014 where we were able to achieve 95% of theoretical density with SS420 stainless steel powder with additional 0.5w% BC, a remarkable achievement considering that about 55% of theoretical density was achieved with traditional 3DP technique.

6. CONCLUSION

We proposed a tile, composed of several shrink-fit materials, in order to produce a buckling action on the assembly of these tiles under a given thermal loading. These tiles, seamlessly fit together, will expand or shrink, exerting forces on the other tiles, causing buckling when heated. The FEM simulation using ABAQUS verified that the model buckled downward by setting the proper design parameters and loading conditions. The successful processing method was the shrink-fitting technique described in this report. It was found that ZrW_2O_8 undergoes a chemical reaction with alumina fibers above 1135 degrees. The reaction compound $Al_2(WO_4)_3$ will change to a liquid phase, which distorts the final sample's shape, compromising the sample. Concerning SiC fibers, although there was no sign of a reaction with ZrW_2O_8, because of its stiffness and large CTE difference, the thermal stress during the sintering has broken the sample. Therefore, it is impossible to combine ZrW_2O_8 with fibers. By using the shrink-fitting technique, several samples were successfully made. ZrW_2O_8 and ZrO_2 tiles with a designed shape were partially sintered and machined, and with the dimension compensation, the perspirable skin assembly was fabricated. After co-sintering the sample, the tile was fabricated by controlling the sintering time.

REFERENCES

1. B. Oguz, L. Sun and P. Kwon, Perspirable Skin: A Multifunctional Material System For Self-Cooling, ASME Conference on Smart Materials, Adaptive Structures and Intelligent Systems, SMASIS2008, October 28-30, 2008, Ellicott City, Maryland, USA
2. Roy, R., Agrawal D.K., MacKinstry H.A., Very low thermal expansion coefficient materials, Annu. Rev. Mater. Sci., 1989, 19, 59-81
3. Mittal, R. and Chaplot S.L., Lattice dynamical calculation of isotropic Negative Thermal Expansion in ZrW2O8 over 0-1050K., Phys. Rev. B, 1999, 60, Bo.10, 7234-7237
4. Evans J.S.O., Mary T.A. and Sleight A.W., Negative thermal expansion material, Phys. B., 1998, 241-243, 311-316
5. Mary, T.A., Evans, J.S.O., Vogt, T. and Sleight, A.W., Negative thermal expansion from0.3 to 1050 Kelvin in ZrW2O8, Science, 1996, 272, 90-92
6. G. Savage, Carbon-carbon composites, New York: Chapman & Hall, pp. 37-80 & pp. 322-332, 1993.
7. Yilmaz, S., Phase transformations in thermally cycled Cu/ZrW_2O_8 composites investigated by synchrotron x-ray diffraction, J. Phys. Cond. Mater., 14, pp. 365-375, 2002
8. M. Taya, and R. Arsenault, Metal Matrix Composites,1st edition, Pergamon Press, 1989.
9. L. Sun, A. Sneller and P. Kwon, "ZrW_2O_8-containing Composites with Near-zero Coefficient of Thermal Expansion Fabricated by Various Methods: Comparison and Optimization," 68, pp. 3425-3430, 2008.

10. L. Sun, X. Shi, A. Sneller, C. Uher and P. Kwon, “In-situ synthesis and thermal properties of ZrO2/ZrW2O8,” The proceeding for 23rd annual technical conference of ASC, pp. 14-23, 2008.
11. L. Sun, and P. Kwon, “ZrW2O8/ZrO2 composites by in situ synthesis of ZrO2+WO3: Processing, coefficient of thermal expansion, and theoretical model prediction”. Material Science and Engineering Vol. A527, pp. 93-97, 2009.
12. I.A.H. Al-Dawery, and E.G. Butler “Fabrication of high-temperature resistant oxide ceramic matrix composites”. Composites Part A, Vol. 32, pp. 1007-1012, 2001.
13. K. Kuribayashi, M. Yoshimura, T. Ohta, and T. Sata. “High-temperature phase relations in the system Y2O3-Y2O3·WO3” Journal of the American Ceramic Society, Vol. 63, No. 11-12, pp. 644-647, 1980.
14. L. Sun and P. Kwon “ZrW2O8–ZrO2 Continuous Functionally Graded Materials Fabricated by In Situ Reaction of ZrO2 and WO3”. Journal of the American Ceramic Society, Vol. 93, No. 3, pp. 703-708, 2010.
15. J.L. Waring “Phase equilibria in the system aluminum oxide/tungsten oxide”. Journal of the American Ceramic Society, Vol. 48, No. 9, pp. 493-493, 1965.
16. Li, S., Kim, Y., Kim, D., and Kwon, P., 2009, “Densification and Properties of 420 Stainless Steel Produced by Three-Dimensional Printing with Addition of Si_3N_4 Powder,” *Journal of Manufacturing Science and Engineering*, **131**, 6, pp. 061001.

Personnel Supported

Patrick Kwon
Mingang Wang (Ph. D. Student)
Truong Do (Ph.D. Student)
Alek Vartanian (Undergraduate student)

Publications.

L. Sun and P. Kwon “ZrW2O8–ZrO2 Continuous Functionally Graded Materials Fabricated by In Situ Reaction of ZrO2 and WO3”. Journal of the American Ceramic Society, Vol. 93, No. 3, pp. 703-708, 2010.

Wang, M., Chen, C.-W., Lempke, M., Wong, T. and Kwon, P., “Design and Processing of Advanced Materials for Perspirable Skin,” 18th International Conference on Composite Materials, Jeju, South Korea.

Wang, M., Lempke, M., Wong, T. and Kwon, P., 2013*, “Perspirable Skin: Thermal Buckling Achieved By Complex Functionally Graded Materials,” Journal of Manufacturing Processes, 15, pp. 121-126.*

T. Do*, C. S. Shin, D. Stetsko, G. VanConant, A. Vartanian, S. Pei & P. Kwon, 2015, ‘Improving Structural Integrity with Boron-Based Additives for 3D printed 420 Stainless Steel, NARMC, Charlotte, North Carolina.

Interactions/Transactions

P. Kwon, 2010, presentation at AFOSR Contractors’ Meeting, Arlington, VA.

P. Kwon, 2011, presentation at International Conference of Composite Materials, Jeju, Korea.

New Discoveries, Inventions or Patent Disclosure

Nothing to report

1.

1. Report Type

F na Report

Primary Contact E-mail

Contact email if there is a problem with the report.

pkwon@egr.msu.edu

Primary Contact Phone Number

Contact phone number if there is a problem with the report

517-355-073

Organization / Institution name

M ch gan State Un vers ty

Grant/Contract Title

The full title of the funded effort.

DEVELOPMENT OF NEW GENERATION OF PERSPIRABLE SKIN

Grant/Contract Number

AFOSR assigned control number. It must begin with "FA9550" or "F49620" or "FA2386".

FA9550-10-1-0238

Principal Investigator Name

The full name of the principal investigator on the grant or contract.

Patr ck Kwon

Program Manager

The AFOSR Program Manager currently assigned to the award

Do. Byung-L p Lee

Reporting Period Start Date

06/15/2010

Reporting Period End Date

11/14/2014

Abstract

Th s research work a ms at the deve opment of the autonomous, se f-coo ng mu t - funct ona mater a systems. S m ar to our sk n that ma nta ns our body temperature, the proposed mater a system w react to the externa heat and open tse f for the purpose of se f-coo ng. Thus, we have co ned the term, Persp rab e Sk n. The autonomous, se f- regu at ng act on of the sk n comes from the nherent, un que capac ty of each mater a n response to a temperature change. The w de spectrum of the changes n a var ety of mater a s s harnessed to create the open ngs for se f-coo ng. In the prev ous y funded program, th s concept ma n y has re ed upon the n-p ane deformat ons on the surface p ane of the sk n and has m ted capac ty for se f-coo ng. Th s proposed work ntends to exp ore the poss b ty of ach ev ng the out-of the p ane deformat on that can expe a much arger vo ume of the compressed gas onboard, thus ach ev ng the h gh capac ty for se f-coo ng. When th s happens, the compressed a r b ankets the surface to prevent fr ct ona heat ng as a s m ar techno ogy was found to be ncred b y effect ve n permanent ho es on turb ne b ade. In part cu ar, three approaches are be ng cons dered to create cons derab e out-of-p ane deformat ons for h gh capac ty of se f-coo ng; (1)

Des gned therma deformat on, (2) Buck ng caused by therma oad ng and (3) A h nged structure tr ggered by nterna pressure. A of these approaches must work w th the therma grad ent oad ng preva ent n such app cat on. At the beg nn ng of the project, the f rst approach has been undertaken w th modest ga n n the coo ng capac ty. Even though the second and th rd approaches requ red prec s on mach n ng capac ty - wh ch the request for DURIP has been d scouraged due to the budgetary constra nt, we were ab e to work on the deve opment of a mater a system for the second approach. In th s approach, a set of ceram c t t es were des gned and fabr cated, wh ch were shr nk-f tted w th n the open ng of the near zero Coeff c ent of Therma Expans on (CTE) mater a s mu at ng Re nforced Carbon-Carbon Compos tes (RCC). These t es made of d fferent mater a s nc ud ng h gh y comp ex grad ent mater a s nduce therma - nduced buck ng oads among the t es under a g ven therma oad ng cond t on. These t es were f tted together to make seam ess connect ons among them just ke the sk n on re-entry veh c es. However, when heated, these t es expand n certa n d rect ons and shr nk n other d rect ons, exert ng forces on one to the others to cause buck ng, wh ch enab e the persp rab e sk n to b ow out the coo er a r onto the surface for se f-coo ng. Th s report ustrates our effort to ach eve the persp rab e sk n.

Distribution Statement

This is block 12 on the SF298 form.

D str but on A - Approved for Pub c Re ease

Explanation for Distribution Statement

If this is not approved for public release, please provide a short explanation. E.g., contains proprietary information.

SF298 Form

Please attach your SF298 form. A blank SF298 can be found here. Please do not password protect or secure the PDF The maximum file size for an SF298 is 50MB.

AFD-070820-035.pdf

Upload the Report Document. File must be a PDF. Please do not password protect or secure the PDF . The maximum file size for the Report Document is 50MB

F na Report.pdf

Upload a Report Document, if any. The maximum file size for the Report Document is 50MB.

Archival Publications (published) during reporting period:

L. Sun and P. Kwon “ZrW2O8–ZrO2 Cont nuous Funct ona y Graded Mater a s Fabr cated by In S tu React on of ZrO2 and WO3”. Journa of the Amer can Ceram c Soc ety, Vo . 93, No. 3, pp. 703-708, 2010.

Wang, M., Chen, C.-W., Lempke, M., Wong, T. and Kwon, P., “Des gn and Process ng of Advanced Mater a s for Persp rab e Sk n,” 18th Internat ona Conference on Compos te Mater a s, Jeju, South Korea.

Wang, M., Lempke, M., Wong, T. and Kwon, P., 2013, “Persp rab e Sk n: Therma Buck ng Ach eved By Comp ex Funct ona y Graded Mater a s,” Journa of Manufactur ng Processes, 15, pp. 121-126.

T. Do*, C..S. Sh n, D. Stetsko, G. VanConant, A. Vartan an, S. Pe & P. Kwon, 2015, Improv ng Structura Integr ty w th Boron-Based Add t ves for 3D pr nted 420 Sta n ess Stee , NARMC, Char otte, North Caro na.

Changes in research objectives (if any):

Change in AFOSR Program Manager, if any:

DISTRIBUTION A: Distribution approved for public release.

Extensions granted or milestones slipped, if any:

The request for f ve month extens on was granted.

AFOSR LRIR Number

LRIR Title

Reporting Period

Laboratory Task Manager

Program Officer

Research Objectives

Technical Summary

Funding Summary by Cost Category (by FY, $K)

	Start ng FY	FY+1	FY+2
Sa ary			
Equ pment/Fac t es			
Supp es			
Tota			

Report Document

Report Document - Text Analysis

Report Document - Text Analysis

Appendix Documents

2. Thank You

E-mail user

Feb 11, 2015 17:07:37 Success: Ema Sent to: pkwon@egr.msu.edu